

Evaluation of the hydrodynamics of high-pressure ebullated beds based on dimensional similitude

J.L. Sánchez^a, R.S. Ruiz^{a,*}, F. Alonso^{b,c}, J. Ancheyta^b

^aDepartamento de Ingeniería de Procesos e Hidráulica, Universidad Autónoma Metropolitana-Iztapalapa, Av. San Rafael Atlixco No. 186, Col. Vicentina, México 09340, D.F., Mexico

^bInstituto Mexicano del Petróleo, Eje Central Lázaro Cárdenas 152, México, D.F., 07730, Mexico

^cInstituto Tecnológico de Ciudad Madero, Juventino Rosas y Jesús Urueta, Col. Los Mangos, Cd. Madero, Tam., 89440, Mexico

Available online 11 December 2007

Abstract

The scale-up method for three-phase fluidized beds hydrodynamics proposed by Safoniuk et al. [M. Safoniuk, J.R. Grace, L. Hackman, C.A. McKnight, Chem. Eng. Sci. 54 (1999) 4961], based upon the principles of dynamic similitude, was tested matching several systems operated at high pressure with model systems operated at atmospheric pressure. Experiments were carried out to test this technique by comparing global phase holdups, and flow regime in systems where the five dimensionless groups proposed by the method were matched, but which were operated at significantly different pressures. The differences observed between the hydrodynamic parameters of the high pressure and model systems suggest that the five dimensionless groups employed are not enough to fully characterize the global bed behavior. Similar findings have been reported by Macchi et al. [A. Macchi, H. Bi, J.R. Grace, C.A. McKnight, L. Hackman, Chem. Eng. Sci. 54 (2001)] based on differences observed in the local dynamic bed behavior between systems operated at atmospheric pressure.

© 2007 Elsevier B.V. All rights reserved.

Keywords: Ebullated bed; Hydrodynamics; Scaling; Similitude; High pressure

1. Introduction

Ebullated beds are three-phase gas–liquid–solid fluidized beds which differ from slurry bubble columns in that their particles are sufficiently large so as to behave as a distinct third phase. Ebullated bed reactors operated under high pressures and high temperatures are applied industrially in the upgrading of heavy oil and high molecular weight feedstocks. Knowledge of the hydrodynamic behavior at high pressure and temperature is critical in predicting the bed performance as a chemical reactor. The operating pressure has been found to have a significant effect on the hydrodynamics of these three-phase systems [1–3]. Higher pressures yield smaller bubbles and more uniform bubble-size distribution, and thus higher gas velocities are required for the transition between the dispersed and coalesced bubble flow regimes. Since the hydrodynamics control the degree of fluids–solids contact, thorough understanding of the

hydrodynamic properties is essential to eliminate significant scale-up effects.

Some difficulties exist in scaling-up the results from small laboratory equipment to the extreme operating conditions of large industrial units. For two-phase systems, much work has been carried out to solve scaling problems [4–6] but comparatively little has been published regarding the application of scaling laws to three-phase systems. With the aid of the Buckingham Pi theorem, Safoniuk et al. [7] proposed a method of scaling hydrodynamics in three-phase fluidized beds based on achieving geometric and dynamic similitude which resulted in basically five dimensionless groups:

$$M = \frac{g \Delta \rho \mu_1^4}{\rho_1^2 \sigma^3}, \quad \text{Morton number;} \quad (1)$$

$$Eo = \frac{g \Delta \rho d_p^2}{\sigma}, \quad \text{Eötvös number;} \quad (2)$$

$$Re_1 = \frac{\rho_1 d_p U_1}{\mu_1}, \quad \text{liquid Reynolds number;} \quad (3)$$

* Corresponding author. Tel.: +52 5804 4648; fax: +52 5804 4900.

E-mail address: rmr@xanum.uam.mx (R.S. Ruiz).

Nomenclature

A	column cross-sectional area (m ²)
d_p	particle diameter (m)
D_c	column diameter (m)
Eo	Eötvös number ($= g \Delta \rho d_p^2 / \sigma$)
g	gravitational acceleration (9.8 m/s ²)
H	expanded bed height (m)
L	length (m)
M	Morton number ($= g \Delta \rho \mu_1^4 / (\rho_1^2 \sigma^3)$)
P	pressure (Pa)
ΔP	pressure drop (Pa)
Re_g	$Re_1 \times \beta_U = \rho_1 d_p U_g / \mu_1$
Re_1	liquid Reynolds number ($= \rho_1 d_p U_1 / \mu_1$)
T	temperature (°C)
U	superficial velocity (m/s)
W_s	particle inventory (kg)
Δz	difference in axial height (m)

Greek letters

β_d	ratio of densities ($= \rho_p / \rho_l$)
β_U	ratio of superficial velocities ($= U_g / U_l$)
$\Delta \rho$	bouyancy term ($= \rho_l - \rho_g$) (kg/m ³)
ε	holdup
μ	viscosity (Pa s)
ρ	density (kg/m ³)
σ	surface tension (N/m)

Subscripts

b	bubble
g	gas
l	liquid
p	particle

$$\beta_d = \frac{\rho_p}{\rho_l}, \quad \text{density ratio; and} \quad (4)$$

$$\beta_U = \frac{U_g}{U_l}, \quad \text{superficial velocity ratio.} \quad (5)$$

The authors compared gas holdup and bed expansion in two different columns operating with significantly different liquid and solid properties with close matching of the five dimensionless groups. They reported good agreement between both units for most of the data. Macchi et al. [8] tested the scaling approach proposed by Safoniuk et al. [7] using two matched systems, where aqueous glycerol solution and silicone oil were utilized respectively as the liquid phase of each unit. They compared statistically hydrodynamic parameters such as bed expansion, gas holdups, dimensionless transition velocities between dispersed and coalesced bubble flow regimes, and the minimum liquid fluidization velocity Reynolds number, and reported that although the differences between the hydrodynamic parameters for the two systems studied were found to be statistically significant, they were also generally small and less than 12%. They attributed the mismatch to differences in

the coalescing behavior of the water–glycerol mixture and that of a pure monocomponent liquid as silicone oil. It should be noted that both of these works have evaluated the scaling approach proposed by Safoniuk et al. based on systems operated at atmospheric pressure.

In the present work, the dimensional similitude approach proposed by Sofaniuk et al. [7] is tested in simulating the hydrodynamics of a three-phase fluidized bed operated at high pressure using a model system at atmospheric pressure and for both of which the five dimensionless groups (Eqs. (1)–(5)) are closely matched.

2. Experimental

In order to evaluate the fundamental approach to simulate bed and bubble hydrodynamics in high-pressure, high-temperature industrial units using small-scale cold-flow models, it is important that accurate industrial data with which to compare the laboratory results are used. In the present work, adequate industrial data were not available for this purpose, however, hydrodynamic data for a high-pressure laboratory unit reported by Luo et al. [9] was considered as suitable and hence was chosen as the prototype or reference system. This system consisted of a stainless-steel column with an inner diameter of 0.051 m and a 0.8 m total height. Paratherm NF heat-transfer fluid and nitrogen were used as the liquid and gas phases, respectively. Hydrodynamic data are reported in this reference for 3 mm spherical glass beads ($\rho_s = 2520 \text{ kg/m}^3$) used as the solid phase, for a constant operating bed temperature of 34 °C, and pressures up to 15.6 MPa. The physical properties of the gas and liquid phases at various pressures, required for the calculation of the dimensionless groups were also reported [9].

The experimental unit employed for simulating the prototype system (referred to as the model system) is shown schematically in Fig. 1. A cylindrical glass column of 0.1 m internal diameter and 1.4 m height was used. The column is made of three sections, namely, the gas–liquid distributor

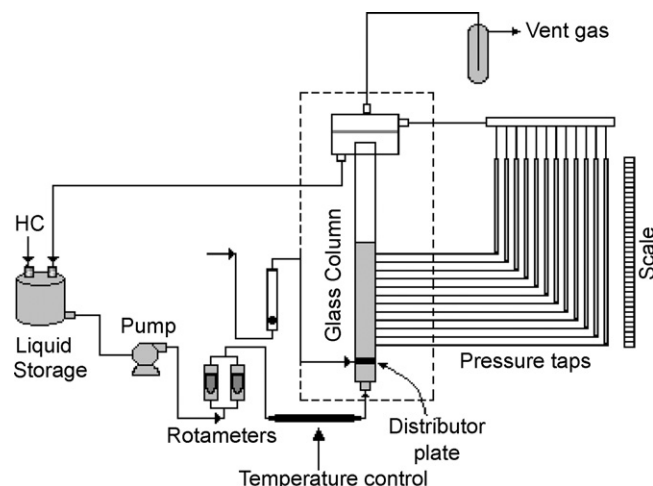


Fig. 1. Schematic diagram of experimental model system.

[illegible]

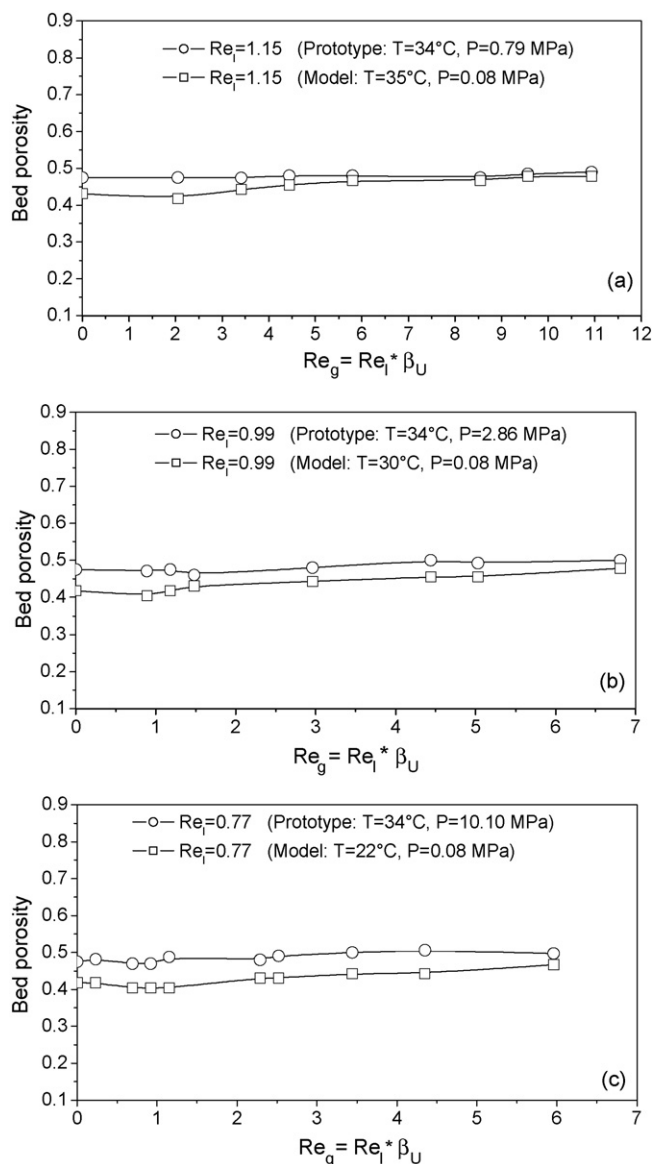


Fig. 2. Bed porosity versus Re_g for prototype and model systems with the former operated at three different pressures: (a) 0.79 MPa, (b) 2.86 MPa, and (c) 10.10 MPa.

3.1. Bed porosity

Bed expansion characteristics or the bed porosity has been studied under high-pressure conditions [2,3,9] and it has been reported that, in general, bed porosity is more sensitive to the liquid than to the gas velocity. It has also been found that, at a given liquid velocity, upon introduction of the gas phase the bed porosity can either decrease or increase depending on the bubble flow pattern. The bed porosities for the prototype, for different operating conditions, and for the corresponding model systems are shown in Figs. 2 and 3. Fig. 2 presents the variation of the bed porosity of the prototype with gas Reynolds number for three different operating pressures, 0.79, 2.86, and 10.10 MPa, and for an average liquid Reynolds number of 0.97. It is clear from this figure, for all three pressures, that an increase in the gas Reynolds number increases slightly the bed

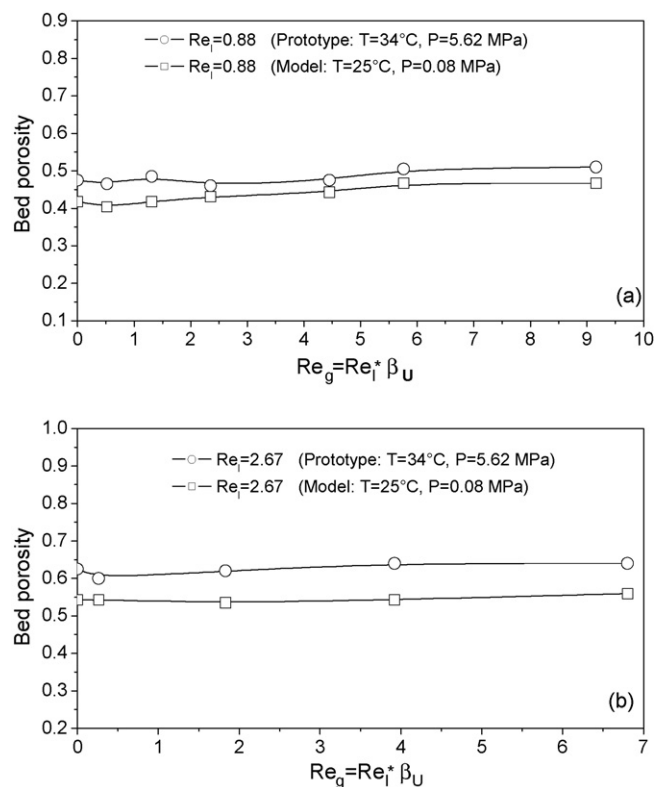


Fig. 3. Bed porosity versus Re_g for prototype and model systems with the former operated at 5.62 MPa and both systems at: (a) $Re_l = 0.88$ and (b) $Re_l = 2.67$.

porosity of the prototype system and that bed contraction was not evident from the data. Fig. 2 also shows the results obtained with the corresponding matching model system. As can be seen, a reasonable correspondence between the values of the prototype and the model appears to have been obtained, especially for the prototype operated at lower pressures. For all the data in Fig. 2 the deviations between porosities were found to be within the 2–14% range. It is also evident that the general effect of gas velocity on the model bed porosity was qualitatively similar to those reported for the prototype. The effect of liquid velocity on bed porosity for the model and prototype systems is shown in Fig. 3, for the prototype operated at a pressure of 5.62 MPa. It is clear that both the prototype and the model responded similarly to the increase in the liquid Reynolds number although the bed porosities were comparatively lower for the latter.

From the above results it should be pointed out that although the observed similarities, the prototype system showed systematically higher bed porosities than those for the matching model. This difference could be due to the foaming character of the liquid utilized in the model system, which during the operation showed a tendency to trap small air bubbles that could have the effect of diminishing the effective viscosity of the continuous phase and hence the drag force on the particles.

3.2. Gas and liquid holdups

It has been reported in the literature that the gas and liquid holdups in three-phase fluidized beds can be affected by the

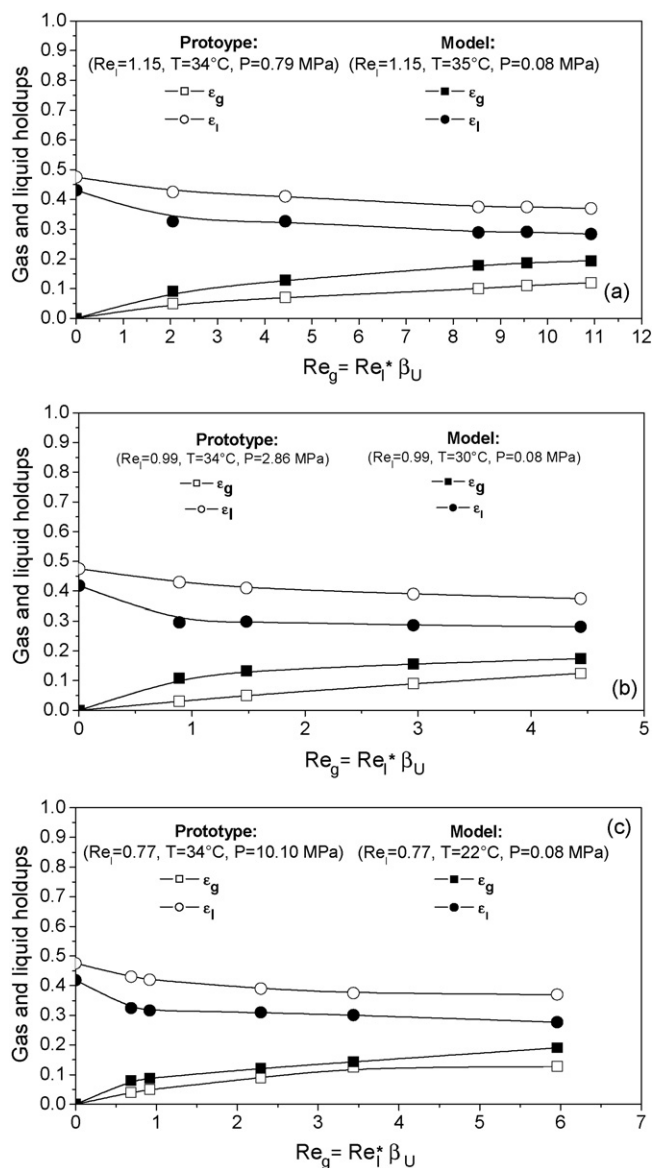


Fig. 4. Gas and liquid holdups versus Re_g for prototype and model systems with the former operated at three different pressures: (a) 0.79 MPa, (b) 2.86 MPa, and (c) 10.10 MPa.

operating pressure through its effect on the bubble characteristics and on the flow regime [1,9]. An increase in pressure at constants gas and liquid velocities produces a reduction of the size and velocity of the gas bubbles which in turn increases the gas holdup in the fluidized bed.

The bed gas and liquid holdups for the prototype, for different operating conditions, and for the corresponding model systems are shown in Figs. 4 and 5. Fig. 4 presents the variation of the holdups for the prototype with gas Reynolds number for three different operating pressures, 0.79, 2.86, and 10.10 MPa, and for an average liquid Reynolds number of 0.97. A continuous increase in gas holdup is observed with an increase in gas Reynolds number, which seems to be more pronounced at higher pressures. The liquid holdup, on the other hand, decreases with an increase of gas flow rate and operating pressure. The gas and liquid holdups for the corresponding

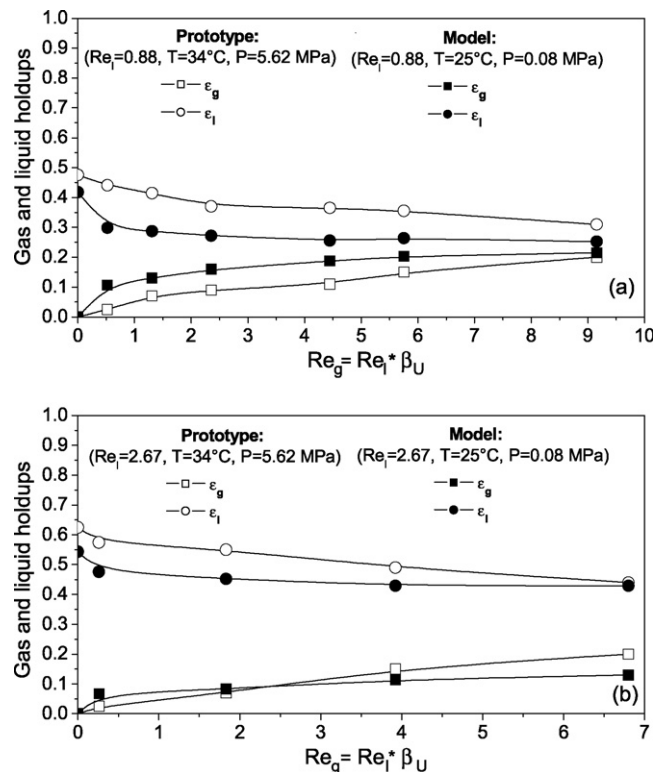


Fig. 5. Gas and liquid holdups versus Re_g for prototype and model systems with the former operated at 5.62 MPa and both systems at: (a) $Re_l = 0.88$ and (b) $Re_l = 2.67$.

matching model systems are also shown in Fig. 4. For all three cases shown the gas holdup of the model increases with gas velocity and does so with values higher than for the corresponding prototype system. For the liquid holdups, the model systems show a qualitatively similar behavior to those observed for the prototype systems, however they were always found to be smaller than the latter. The larger gas holdups obtained for the model can be attributed to the noncoalescing behavior of the oil fraction employed for such systems, and in which gas bubbles tend to rise as small and slow entities that produce relatively high gas holdups. On the other hand, Paratherm NF heat transfer liquid was employed in the prototype system and for which no foaming behavior has been reported [2,9,11].

The effect of liquid velocity on gas and liquid holdups for the model and prototype systems is shown in Fig. 5, for the prototype operated at a pressure of 5.62 MPa. The gas holdups for the prototypes are found to decrease slightly with the increase in liquid velocity. Similarly, the gas holdups for the models also decrease with liquid velocity, but does so at larger rates than in the prototypes, and this is particularly noticeable at high gas velocities for which the gas holdups of the prototypes exceed those of the models. Luo et al. [9] reported that the pressure effect on gas holdup is more pronounced at high gas velocities. As gas velocity is increased larger bubbles can be expected to occur and hence the effect of pressure on bubble breakup phenomena becomes more evident. From comparison of the gas holdups for the prototype and the model systems it seems that the response of the prototype at high pressure and

fluid velocities is reproduced only partially by the model system. It has been reported that pressure affects the hydrodynamics through the variation on the physical properties of the gas and liquid phases, therefore, in the prototype both the gas and the liquid are being affected. On the other hand, the model system was designed based on the five dimensionless groups presented in Eqs. (1)–(5), none of which considers the properties of the gas phase. For the prototype operated at high pressure and gas flow rates it therefore seems necessary to utilize the extra dimensionless group suggested by Safoniuk et al. [7] given by the gas to liquid density ratio, ρ_g/ρ_l .

3.3. Flow regime

The transition between the dispersed and coalesced bubble regimes in high-pressure ebullated beds has been analyzed by many researchers utilizing the gas drift flux concept [3,9] The gas drift flux, j_{cd} , for three-phase fluidized beds can be expressed by [12]

$$j_{cd} = \frac{1 - \varepsilon_g}{\varepsilon_l} (U_{g\varepsilon_l} - U_{l\varepsilon_g}) \quad (9)$$

which seems to increase with gas holdup at a much higher rate at the coalesce bubble flow regime as compared to that at the dispersed bubble flow regime. An increase of pressure has been reported to lead to an increase in the transition gas velocity from the dispersed to the coalesced bubble regimes. The gas drift flux for the prototype operated at different pressures and the corresponding matching model systems are presented in Fig. 6. As can be seen in Fig. 6(a), for the prototype system as pressure is

increased regime transitions occurs at higher bed porosities, and hence at higher gas velocities. The gas drift flux for the model systems is shown in Fig. 6(b), and in which the symbols utilized for the data are the same to those of the prototypes in Fig. 6(a) that are being matched. In order to match the dimensionless groups between the model and the prototype systems the operating temperature of the model systems had to be modified so as to produce the necessary changes in liquid properties. As it is shown in Fig. 6(b) an increase in the transition gas velocities in the prototypes is also qualitatively predicted by the model systems but in the latter it is produced by decreasing the operating temperature.

The prevailing bubble flow regime depends on both the gas and liquid velocities. Fig. 7 shows the gas drift flux for both prototype and model systems at two different liquid velocities for a given prototype pressure of 5.62 MPa. For the range of gas porosities in Fig. 7, and for both liquid velocities the prototype systems seem to operate in the dispersed bubble flow regime. On the other hand, the model systems seem to show different regime transition conditions for the two liquid velocities considered. As the liquid Reynolds number is increased the gas holdup and hence the transition gas velocity decreases. It is then clear from this figure that the prototype systems are maintained in the dispersed bubble flow regime for a broader range of gas and liquid velocities as compared to the matching model systems. The effect of pressure on the hydrodynamics of the prototypes have been modeled in the present work by matching of five dimensionless groups appear to be insufficient when operating at high gas and liquid velocity conditions. Pressure affects hydrodynamics by affecting both liquid and gas

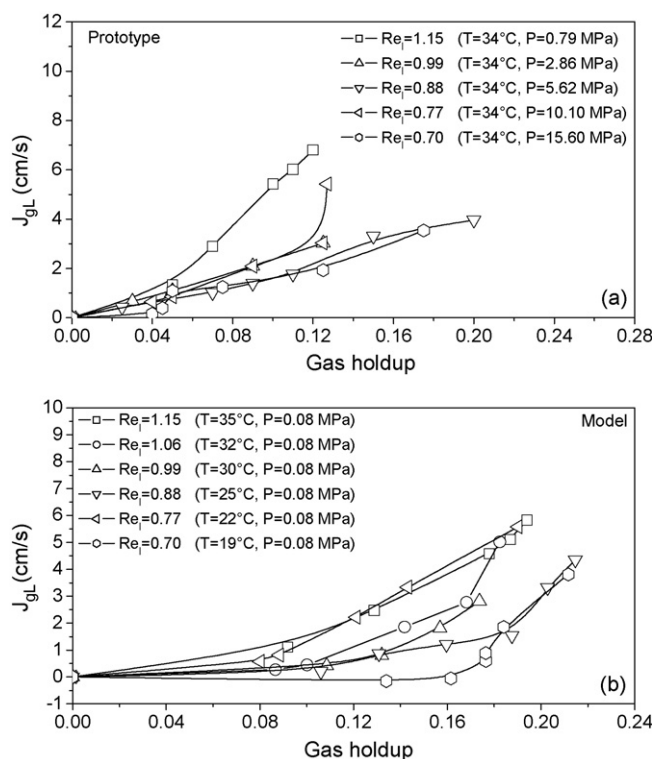


Fig. 6. Gas drift flux versus gas holdup for (a) the prototype systems operated at different pressures and (b) the corresponding matching model systems.

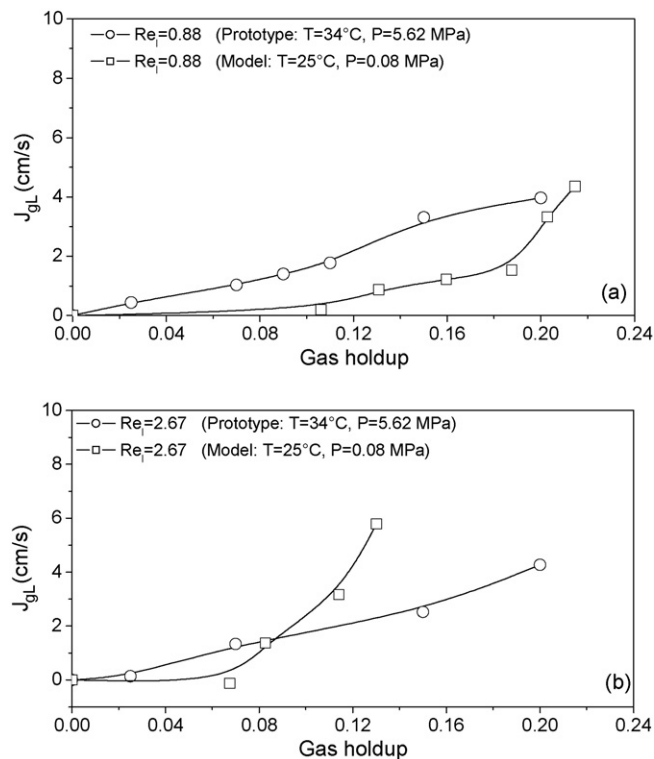


Fig. 7. Gas drift flux for both prototype and model systems with the former operated at 5.62 MPa and both systems at: (a) $Re_1 = 0.88$ and (b) $Re_1 = 2.67$.

Table 2
RMSD and Fm between bed porosities for the matched systems

Matched system	Re_1	RMSD	Fm
I	1.15	0.063	1.055
II	1.06	0.085	1.091
III	0.99	0.093	1.098
IV	0.88	0.101	1.108
	2.67	0.129	1.147
V	0.77	0.126	1.140
	2.34	0.119	1.133
VI	0.70	0.132	1.151
	2.13	0.112	1.121
Mean		0.108	1.115

properties and the aforementioned groups do not consider the gas properties. As mentioned earlier, the use of a denser gas in the model system that would match the densities ratio, ρ_g/ρ_l , could account to the effect of pressure on the gas phase. For the operating conditions considered in Fig. 7, the density ratios for the prototype and model systems were 7.02×10^{-2} and 9.79×10^{-4} , respectively. Therefore, in order to match the density ratio between both units gas with a density of 62.4 kg/m^3 is required for the model system, and which is about two orders of magnitude larger than that of nitrogen at atmospheric pressure and ambient temperature. As can be expected, availability of a safe to use gas with such a density could be a limitation to the exact matching of the density group.

The differences in the hydrodynamic parameters between the prototype and the model systems have been characterized by the root mean standard deviation (RMSD) and bias factor (Fm)

$$\text{RMSD} = \sqrt{\frac{1}{k} \sum_{i=1}^k \left[(\text{prototype} - \text{Model}) / \text{prototype} \right]^2},$$

$$\text{Fm} = \exp \left[\sum_{i=1}^k \ln(\text{prototype} / \text{Model}) \right]. \quad (10)$$

Table 2 presents these quantities for the bed porosity and six different prototype operating pressures (see Table 1). The results show that the differences between prototype and model tend to be smaller for the lower pressure systems and that the largest RMSD obtained corresponds to the matching of the prototype operated at the highest pressure considered (15.6 MPa). It is also evident from this table that Fm is always larger than unity and which means that the bed porosities for the prototype are also always underestimated by the model.

The average RMSD and Fm values obtained for the hydrodynamic parameters for all the matched systems considered are presented in Table 3. The data are clearly skewed ($0.575 < \text{Fm} < 1.284$) and the best RMSD corresponds to the bed porosity, of the order of 0.11, which is followed by that for the liquid holdup, and then, with a significantly large deviation, by the gas holdup.

From the present results it seems that the dimensional similitude approach provides a useful tool for estimation of

Table 3
Average RMSD and Fm between hydrodynamic parameters for the matched systems

Hydrodynamic parameter	RMSD	Fm
Bed porosity	0.108	1.115
Gas holdup	2.107	0.575
Liquid holdup	0.237	1.284

global hydrodynamics but it is clear that they seem to depend on the coalescing nature of the liquids in the prototype and model systems. The gasoil mixture employed in the models showed a noncoalescing behavior and a tendency to foam as temperature was decreased and the liquid velocity increased. This behavior produced significantly larger gas holdups in the models as compared to the prototypes even for relatively low gas Reynolds numbers. It is also apparent that the gas to liquid density ratio is a group that needs to be matched when modeling high-pressure systems, especially under relatively high gas and liquid flow rates for which the effect of pressure becomes more evident. Finally, it is evident that differences between the coalescing behaviors of the liquids of the matched systems play an important role that has to be accounted for in future work when selecting the liquid for the model system.

4. Conclusions

The scale-up method for three-phase fluidized beds hydrodynamics proposed by Safoniuk et al. [7], based upon the principles of dynamic similitude, was tested matching several systems operated at high pressure with model systems operated at atmospheric pressure.

Bed porosities were qualitatively similar for prototype and model systems and the quantitative differences were generally less than 13%, however, such differences appeared to increase as the pressure of the prototype system was increased. In general the gas holdup of the model systems overestimated those for the prototype systems, behavior that seems to be attributed to the foaming character of the oil fraction used in model systems that showed a tendency to accumulate small gas bubbles even at low gas velocities. The drift fluxes calculated for both prototype and model systems showed that, although most of them operated in the dispersed bubble regime, the high-pressure systems appear to have larger gas transition velocities between the dispersed and coalesced flow regimes. It seems that the use of denser gases in the model systems could help extend their respective gas transition velocities.

The differences observed between the hydrodynamic parameters of the high pressure and model systems suggest that the five dimensionless groups employed are not enough to fully characterize the global bed behavior and that, although matching the additional group given by gas to liquid density ratio could probably help to extend the dispersed bubble flow regime in the model system, there is still lack of information regarding the coalescing behavior of the liquids used in the matched systems.

Acknowledgement

The authors thank Instituto Mexicano del Petróleo for the financial support.

References

- [6] T.M. Knowlton, S.B.R. Karri, A. Issangya, *Powder Technol.* 150 (2005) 72.
- [7] M. Safoniuk, J.R. Grace, L. Hackman, C.A. McKnight, *Chem. Eng. Sci.* 54 (1999) 4961.
- [8] A. Macchi, H. Bi, J.R. Grace, C.A. McKnight, L. Hackman, *Chem. Eng. Sci.* 54 (2001) 6039.
- [9] X. Luo, P. Jiang, L.-S. Fan, *AIChE J.* 43 (1997) 2432.
- [10] N. Costa, A. De Lucas, P. García, *Ind. Eng. Chem. Process Des. Dev.* 25 (1986) 849.
- [11] X. Luo, J. Zhang, K. Tsuchiya, L.-S. Fan, *Chem. Eng. Sci.* 52 (1997) 3693.
- [12] R.C. Darton, D. Harrison, *Chem. Eng. Sci.* 30 (1975) 581.
- [13] L.-S. Fan, *Gas–Liquid–Solid Fluidization Engineering*, Butterworths, Boston, 1989.

- [1] P. Jiang, D. Arters, L.-S. Fan, *Ind. Eng. Chem. Res.* 31 (1992) 2322.
- [2] P. Jiang, X. Luo, T.-J. Lin, L.-S. Fan, *Powder Technol.* 90 (1997) 103.
- [3] R.S. Ruiz, F. Alonso, J. Ancheyta, *Catal. Today* 109 (2005) 205.
- [4] M. Horio, A. Nonaka, Y. Sawa, I. Muchi, *AIChE J.* 32 (1986) 1466.
- [5] L.R. Glicksman, M.R. Hyre, P.A. Farrell, *Int. J. Multiphase Flow* (1994) 331.